6776

Spatial transcriptomics of response to tepotinib treatment in a patient with NSCLC

Manon A. Simard[1], Felix Geist[1], Carlos Cabrera[2], Santiago Viteri[2], Joachim Albers[1], Michael Zuehlsdorf[1], Niki Karachaliou[1]

[1]Research Unit Oncology, The healthcare business of Merck KGaA, Darmstadt, Germany;
[2]UOMI Cancer Center, Clinica Mi Tres Torres, Barcelona, Spain

CONCLUSION

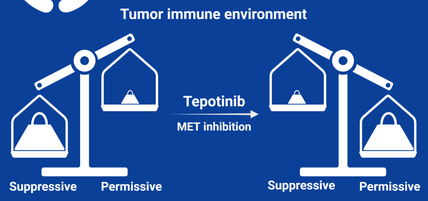

Figure 1: Shifting the balance from an immuno-suppressive to an immuno-permissive tumor environment through tepotinib treatment (generated using BioRender.com).

Neoadjuvant tepotinib treatment in a patient with stage IIIB *METex14* NSCLC resulted in a major pathological response accompanied by a shift to an immuno-permissive and tumor killing environment, based on enriched gene expression profiles. Overall, these spatial transcriptomics results showcase the increased immune cell presence within the tumor along with the down-regulation of immuno-suppressive genes, an increase in cytotoxic T cell activation and upregulation of antigen-presentation processes, all of which could potentially contribute to anti-cancer effects of tepotinib.

BACKGROUND

While cancer therapies are becoming increasingly more targeted, our understanding of the genomic changes occurring during these treatments is mainly lacking. Moreover, tumor heterogeneity and spatial distribution remain important obstacles in predicting tumor evolution and treatment responses. Herein, spatial transcriptomic analysis was used to evaluate the response of NSCLC with *METex14* skipping alteration to neoadjuvant treatment with tepotinib, a highly selective and potent MET class Ib inhibitor. Tepotinib is currently approved for the treatment of patients with NSCLC with *METex14* skipping alterations.

METHODS

GeoMx® digital spatial profiler (DSP; Nanostring Technologies) analysis was conducted on 5 µm thick FFPE sections from paired baseline and on-treatment patient samples. Regions of interest (ROI) were selected by SYTO13 (nuclear), TTF-1 (lung adenocarcinoma), CD3 (T cells) and CD33 (myeloid-derived suppressor cells) morphology markers, with the latter three conjugated to AF555, AF594 & AF647, respectively using Abcam kits. Next-generation sequencing (NGS) was performed on isolated probe barcodes from the Cancer Transcriptome Atlas RNA panel (>1,800 cancer-related genes) supplemented with probes for *METex14*, *CEACAM5*, *CEACAM6*, *CLDN* var1 & *CLDN* var2 using a NovaSeq6000. Technical and biological quality checks were conducted on NGS results prior to third quartile normalization and statistical analysis. Unless otherwise specified, a linear mixed model with Benjamini-Hochberg correction was used to determine significantly altered gene expression. Spatial deconvolution was performed within the GeoMx analysis suite followed by k-means clustering using in-house R scripts.

RESULTS

I. Neoadjuvant tepotinib treatment in a patient with *METex14* NSCLC

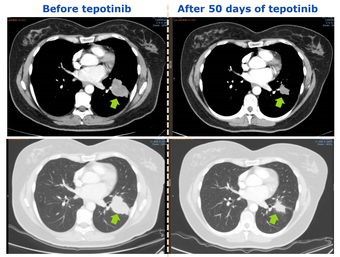

Figure 2: Clinical images of neoadjuvant tepotinib treatment highlighting reduction of tumor size by prior to tumor resection. Major pathological response was observed (< 10 % residual viable tumor cells) and tumor was downstaged from IIIB to IA1.[1]

II. Immune environment of tepotinib treated NSCLC *METex14*

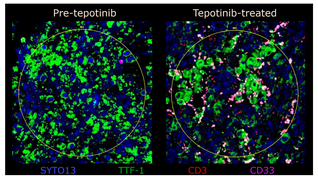

Figure 3: Representative tumor ROIs from both pre-tepotinib and tepotinib-treated biopsies with morphology markers (ROI n = 15 & 79, respectively). Circular ROIs of 250 µm in diameter were selected across all tumor and peripheral regions, to capture the tissue heterogeneity in one FFPE section per biopsy.

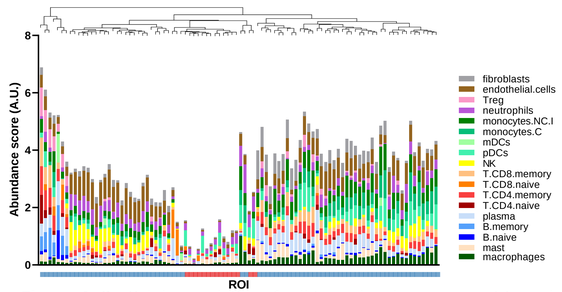

Figure 4: Spatial deconvolution of cell type abundances present in each ROI. A clear distinction between ROIs taken prior to (red) and following (blue) tepotinib treatment can be detected, highlighting the more immuno-permissive milieu present when MET is inhibited.

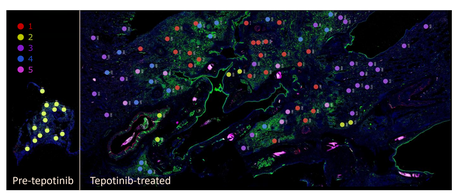

Figure 5: k-means clustering of spatially deconvoluted cell types of ROIs. In the pre-tepotinib tumor the ROIs cluster together spatially as well as from their cell type composition, while ROIs in the tepotinib-treated sample differ substantially in their cell type composition and the tumor is divided into three clusters.

III. Spatial transcriptomics of tepotinib treatment reveal increased antigen-presentation and T cell cytotoxicity

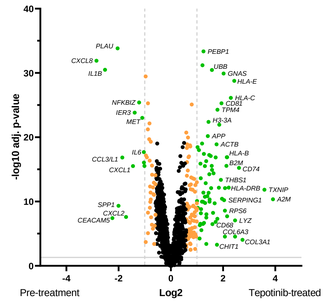

Figure 6: Volcano plot of significantly altered gene expression in neoadjuvant tepotinib-treated *METex14* NSCLC (green: > 2-fold, orange: > 1.5-fold).

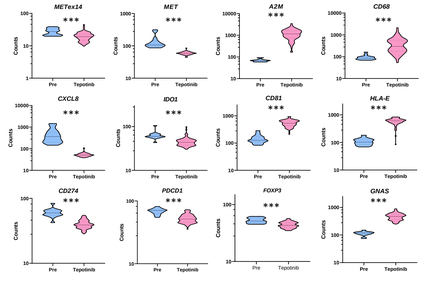

Figure 7: Violin plots of select normalized transcript counts in a patient prior to and following tepotinib treatment demonstrating the shift to a more immuno-permissive tumor and environment (BH multiple correction adjusted p-value; ***, p < 0.05).

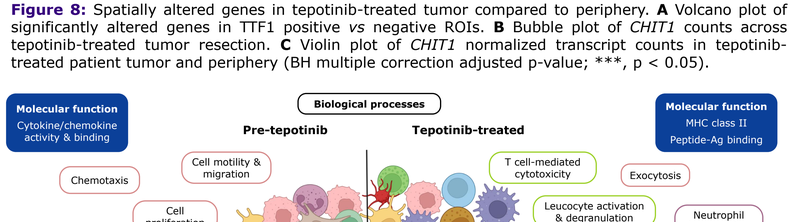

Figure 8: Spatially altered genes in tepotinib-treated tumor compared to periphery. **A** Volcano plot of significantly altered genes in TTF1 positive *vs* negative ROIs. **B** Bubble plot of *CHIT1* counts across tepotinib-treated tumor resection. **C** Violin plot of *CHIT1* normalized transcript counts in tepotinib-treated patient tumor and periphery (BH multiple correction adjusted p-value; ***, p < 0.05).

Figure 9: Schematic of tumor microenvironment and changes occurring under tepotinib treatment based on gene ontology results[2] from significantly altered genes more than 1.5-fold prior to and following tepotinib treatment; biological processes, molecular functions and cellular components involvement are shown for each patient sample. Figure was generated using BioRender.com.

References

1. Cabrera=Gálvez, C. & Viteri-Ramirez, S. *Submitted.*
2. *GOrilla*: http://cbl-gorilla.cs.technion.ac.il

Acknowledgements: The authors would like to thank Jürgen Schmidt and Florian Orio for their technical assistance and input during sample preparation.

Presented at the American Association for Cancer Research Annual Meeting | April 14-19, 2023 | Orlando, Florida, USA

Manon A. Simard
Postdoctoral Researcher, Translational Research
The healthcare business of Merck KGaA, Darmstadt, Germany
manon.simard@emdgroup.com